PREPRINT UCRL- 79880

CONF-771029--49

Lawrence Livermore Laboratory

DESIGN OF AN ELECTROSTATIC END-PLUGGED PLASMA-CONFINEMENT DEVICE

MASTER

R. W. Moir, T. J. Dolan, and W. L. Barr

September 27, 1977

This paper was prepared for inclusion in the Proceedings of the Seventh Symposium on Engineering Problems of Fusion Research, Knoxville, Tennessee, October 25-28, 1977.

This is a preprint of a paper intended for publication in a journal or proceedings. Since changes may be made before publication, this preprint is made available with the understanding that it will not be cited or reproduced without the permission of the author.

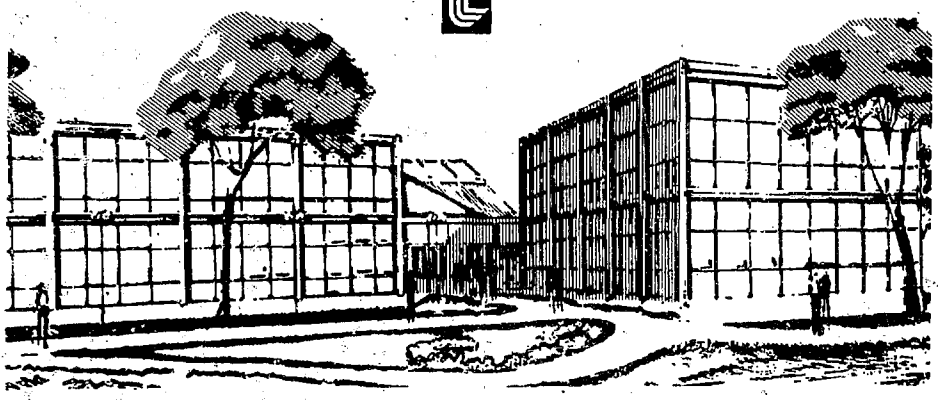

DISTRIBUTION OF THIS DOCUMENT IS UNLIMITED

DESIGN OF AN ELECTROSTATIC END-PLUGGED PLASMA-CONFINEMENT DEVICE*

R. W. Moir, T. J. Dolan,† and W. L. Barr

Lawrence Livermore Laboratory, University of California
Livermore, California 94550

NOTICE
This report was prepared as an account of work sponsored by the United States Government. Neither the United States nor the United States Energy Research and Development Administration, nor any of their employees, nor any of their contractors, subcontractors, or their employees, makes any warranty, express or implied, or assumes any legal liability or responsibility for the accuracy, completeness or usefulness of any information, apparatus, product or process disclosed, or represents that its use would not infringe privately owned rights.

Summary

A laboratory-scale experimental device having an outside diameter of 1.2 m has been designed to test the idea of electrostatic end plugging of an open-ended magnetic-field configuration. The configuration is a toroidal quadrupole having four very thin (<1-mm-thick) line cusps produced by four circular copper coils. Iron is used to concentrate the magnetic flux density to 2.0 T; without the use of iron, the power consumption, which is about 1 MW, would be about 25 times higher. The use of iron also produces a precisely known magnetic field and allows good access for diagnostics and pumping. Iron is also used for both the flux return path and the vacuum chamber. A hollow anode with an adjustable (nominally 1-mm-wide) gap is biased from 10 to 20 kV. Plasma densities of about 10^{13} cm^{-3} and temperatures of about 1 keV might be produced by an electron beam and by electron cyclotron resonance heating. Higher-order multipoles (hexapoles and octopoles) also are described.

Introduction

In open-ended magnetic-confinement systems, the confinement times are determined by the rate at which ions are lost along the open field lines. The concept of electrostatic plugging suggested and developed by Lavrent'ev[1] is one means of reducing this loss rate, thus enhancing the Q (where Q = fusion power/injection power). Other means being studied include the tandem mirror concept, the field-reversed mirror concept, and radio-frequency (rf) plugging.

In electrostatically plugged, open-ended, magnetic-confinement systems, the ions are confined electrostatically in a negative electrostatic potential well produced by the electrons. The electrons are confined by a minimum-B magnetic well, and electron loss along field lines is impeded by the plugging electrodes.

The concept of end-loss reduction by electrostatic plugging has recently been reviewed by Dolan.[2] He discusses the work by Lavrent'ev and coworkers at Khar'kov, by Stansfield, Larsen and Gregory at Quebec, and theoretical work by Ware and others.

The geometry considered here (see Figs. 1 and 2) consists of a toroidal magnetic quadrupole with electrodes for electrostatic plugging at all four line cusps.[3] All previous experiments on electrostatic plugging have been strongly affected by losses at point cusps, which are avoided in this device. For line cusps, the flux bundle and therefore the leakage plasma are much thinner. As a consequence, the applied electrostatic potential can more easily penetrate the line cusp.

Figure 3 shows a suggested experimental device. A high positive voltage (10 to 20 kV) is applied to the anodes [item (4)] and a large negative voltage is applied to the cathodes [item (2)]. When a plasma is produced in the central region, ions are easily lost along magnetic field lines at first, but electrons are repelled by the negative cathode. After the loss of a small fraction of the ions, the slight charge imbalance drives the plasma potential negative relative to the anodes, and a potential barrier ϕ_i is developed that

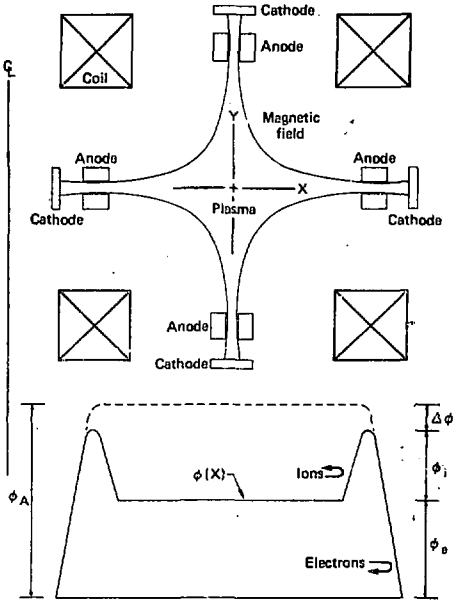

Fig. 1. Electrostatic plugging system and resultant potential distribution. Dashed line shows potential $\phi(x)$ without plasma.

*Work performed under the auspices of the U.S. Energy Research and Development Administration under contract No. W-7405-Eng-48.

†Present address, University of Missouri, Rolla, Missouri.

DISTRIBUTION OF THIS DOCUMENT IS UNLIMITED

Fig. 2. Perspective view of the electrostatic plugging system.

impedes loss of the remaining ions. The electrons exiting along field lines are repelled by the barrier ϕ_e (see Fig. 1). The magnitudes of these two potential barriers adjust so that the electron and ion loss rates are equal.

There is a potential depression $\Delta\phi$ inside the anodes due to the presence there of electron space charge. This potential drop can be satisfactorily small if the thickness of the electron stream in the anodes is of order a Debye length. The converging magnetic field lines tend to make the width of the electron stream from the central field-free plasma region a few electron Larmor radii thick.

The electron density in the anode regions is limited by the diocotron instability so that $\omega_p^2/\omega_{ce}^2 \leq 0.2$, where ω_p is the plasma frequency and ω_{ce} is the electron cyclotron frequency. This limitation results in central plasma densities that are proportional to B^2, with $n = 5 \times 10^{12}$ cm^{-3} at $B = 1.0$ T. The ion temperature measured by the Khar'kov group is roughly one-tenth the applied voltage ϕ_A at low pressures (less than 10^{-6} Torr). If ϕ_A is large enough, the electron energy loss along magnetic field lines will be negligible in comparison with energy loss across the magnetic field.

Where cross-field transport is dominated by electron-ion collisions, the confinement parameter is given by

$$n\tau = n\tau_{ei}\frac{V}{A\rho_{e0}}N$$

$$= 3.3 \times 10^{18}\, r_p B_0 T_e N,$$

where n is the central ion density, B_0(T) is the magnetic field at the edge of the plasma, T_e(keV) is the electron temperature, r_p is the plasma minor radius in metres, V is the plasma volume, A is the plasma surface area, ρ_{e0} is the electron gyroradius in the field B_0, N is the number of local electron gyroradii across the boundary layer, and τ_{ei} is the electron-ion scattering time.

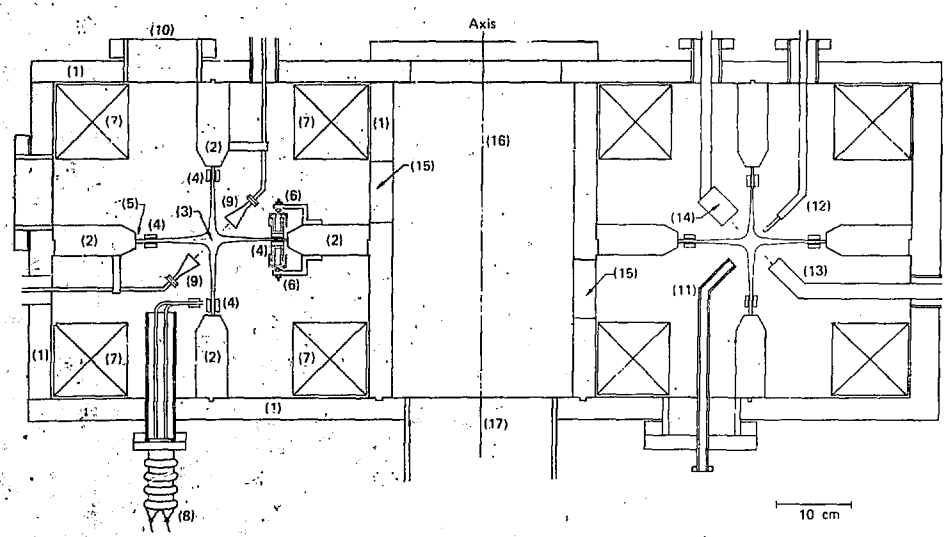

Fig. 3. Experimental device, showing (1) iron vacuum chamber and magnetic flux path, (2) iron magnet pole faces, (3) plasma, (4) anodes, (5) electron-gun filament, (6) anode support insulators, shield, and adjustment screws, (7) magnet coils, (8) anode cooling water and high-voltage feedthrough, (9) microwave interferometer, (10) viewports, (11) 10-GHz rf heating waveguide, (12) movable limiter probe, (13) heavy ion beam source, (14) ion-beam detector, (15) vacuum pumping ports, (16) inner chamber, and (17) ionization pump.

Typical parameters are given in Table 1 for this device along with comparative values for an experimental device at Khar'kov and with those for an example reactor design.[4]

Experiments on a device such as described here would have four main physics objectives: to study (1) phenomena in the boundary layer including cross-field transport, (2) potential well maintenance, (3) scaling relations, and (4) impurity effects. These phenomena are important because they determine the density limit.

Boundary Layer Phenomena

Particle transport rates, electron density distribution, and electric field fluctuations in the boundary layer and anode regions must be measured in order to ascertain the effects of diocotron oscillations, two-stream interactions, drift waves, and so on.

Potential Well

The key to hot-ion confinement with electrostatic plugging is creation and maintenance of a deep, negative, electrostatic potential well. Measurements are needed of well depth as a function of applied voltage, magnetic field strength, neutral gas pressure, and heating power (electron-beam or rf heating). The data can be compared with theoretical predictions based on the idea that the depth of the potential well is fixed by the equality of electron and ion loss rates.

Scaling Relations

A check of the scaling relations for density, temperature, and confinement time, as discussed above, must be made. To do this, it will probably be necessary to extend the realm of measurement to higher densities, temperatures, and confinement times than have been obtained so far. The scaling laws to be verified are:

$$n_i \propto B_A^2 ,$$

$$T_i \propto \phi_A ,$$

$$n\tau \approx \left(\frac{r_p}{\rho_{e0}}\right) n\tau_{ei} N ,$$

where n_i is the central ion density, B_A is the magnetic field at the anode, T_i is the ion temperature, and ϕ_A is the anode potential.

Impurity Effects

It should be possible to measure spectroscopically the time variation of the impurity content of the plasma. To minimize impurities, the experiment should have a bakable vacuum system with a comparatively high pumping speed.

Description of the Device

A general description of the main features of the device shown in Fig. 3 will be given here. See Table 2 for a listing of the main parameters.

Magnet Design

The circular quadrupole field is generated by four circular coils (Fig. 3). Adjacent coils carry current in opposite directions. Iron is used for a number of purposes. For example, it provides a flux return path

Table 1. Parameters of various experiments.

	Khar'kov device[a]	Suggested device	Reactor[b]
Magnetic field at the anodes, B (T)	1.0	1.6	7.0
Applied voltage, ϕ_A (kV)	7	10	300
Gas pressure, p (Torr)	10^{-7}-10^{-6}	10^{-7}-10^{-6}	10^{-7}-10^{-6}
Central electron density, n_e (cm^{-3})	5×10^{12}	10^{13}	10^{14}
Electron temperature, T_e (keV)	2	2	30
Ion temperature, T_i (keV)	1	1	20
Energy confinement time, τ_E (ms)	5	10	>1000
Electron-electron scattering time, τ_{ee} (ms)	0.3	0.2	0.9

[a]From Ref. 2.

[b]From Ref. 4.

Table 2. Main parameters of the electrostatic end-plugged plasma-confinement device.

Parameter	Value
Geometry: toroidal multipole cusp with four cusps; chamber outside radius	60 cm
Applied voltage	10 to 20 kV
Anode gap width	1 to 2 mm
Distance from plasma center to cathodes	10 cm
Major radius of plasma	36 cm
Minor radius of plasma	~1 cm
Heating methods	Electron beam; electron cyclotron resonance heating
Plasma parameters:	
Density	10^{13} cm^{-3}
Ion temperature	1 to 2 keV
Confinement time	5 to 10 ms
Plasma volume	1000 cm^3
Electron Larmor radius (taking $T_e \approx 2$ keV) at plasma boundary ($B_0 = 0.11$ T)	~1.4 mm
in anode gap ($B = 1.6$ T)	~0.094 mm
Ion Larmor radius — not applicable, since ions are electrostatically reflected. (In the absence of the electrostatic barrier, $\rho_i \approx 4$ cm at the plasma boundary and ~2.8 mm in anode region for $T_i \approx$ keV).	
Debye length (taking $T_e \approx 2$ keV):	
At plasma boundary ($n \approx 10^{13}$ cm^{-3})	~0.074 mm
In anode gap ($n \approx 3 \times 10^{12}/cm^{-3}$)	~0.13 mm

and concentrates the flux at the specially shaped, high-field-alloy (Fe-Co) pole face. For the same field at the anodes and the same coil size (equal diagnostic access), in the presence of iron the power consumption is reduced by a factor of 25; stated conversely, for the same power, a five times higher field is produced. Because the device is axisymmetric, the iron parts can be machined on a lathe, the result being a precisely known and controlled magnetic field. The iron is also used for the vacuum chamber. If the field is kept below the saturation value in the iron, this chamber can have rather large ports bored through it. These large ports provide good access for plasma production, for heating, for diagnostics, and for pumping.

The pole tip could be made of iron-cobalt alloy, which has a saturation field strength of about 2.4 T. The remainder of the pole and flux return path would be made of magnet iron with the field strength kept below its 2.1-T saturation field strength. A field of about 2 T on the pole face is needed to obtain the design goal of 1.6 T in the anode gap and thus allow the testing of the scaling laws at higher field strength than ever before.

The number of ampere turns (NI) of each coil has been estimated to be 240 kA turns from the formula $NI = \oint d\vec{l}\cdot\vec{B}/\mu$, where μ is the permeability of iron, where the field is assumed to be linear from the center to the pole face (a distance of 10 cm), and where $\mu \gg \mu_0$ everywhere else. The average current density in each coil with 150-cm^2 cross section is 1600 $A\cdot cm^{-2}$. This is based on a 13-cm by 13-cm coil, which is slightly larger than the 10-cm by 10-cm coil shown in Fig. 3 [item (7)]. The power consumed by each small-radius coil is 0.13 MW and by each large-radius coil is 0.3 MW, giving a total magnet power of 0.9 MW.

Vacuum System

The plasma chamber shown in Fig. 3 [item (1)] has a volume of 0.4 m^3. The walls are polished and nickel-plated; all-metal, bakable seals are used throughout. The chamber is evacuated through 16 ports [marked (15) in Fig. 3], each having a conductance for H_2 of about 1500 $l\cdot s^{-1}$, giving a conductance of 24,000 $l\cdot s^{-1}$. Pumping by Ti gettering or cryocondensation can be provided for the inner chamber. Also, a 400 $l\cdot s^{-1}$ ionization pump is located as shown on Fig. 3 [item (17)]. The base pressure should be in the 10^{-9}-Torr range.

During operation, the vacuum pumps run continuously. The plasma is fueled by four thin, gas jets equally spaced azimuthally around the torus and aimed into the plasma. Gas jets are used to keep the gas pressure outside the plasma low.

For the predicted plasma parameters (see Table 2) of a volume of 1000 cm^3, a density of 10^{13} cm^{-3}, and a 5-ms confinement time, 10^{18} H_2 molecules/s will maintain the plasma. Only some of these molecules need be supplied by the gas jet; the remainder will be supplied by wall reflux.

The electron gun is illustrated in Fig. 4. A 0.13-mm-diam thoriated tungsten-wire filament is secured in tension between ceramic tubes mounted in a thin slot at various locations around the outermost iron cathode pole. The ceramic tubes are held in place by wires pulled back through holes in the pole faces. The required gun current is about 160 mA at 10 kV, or about 0.6 mA/cm of filament. Holding 10 to 20 kV

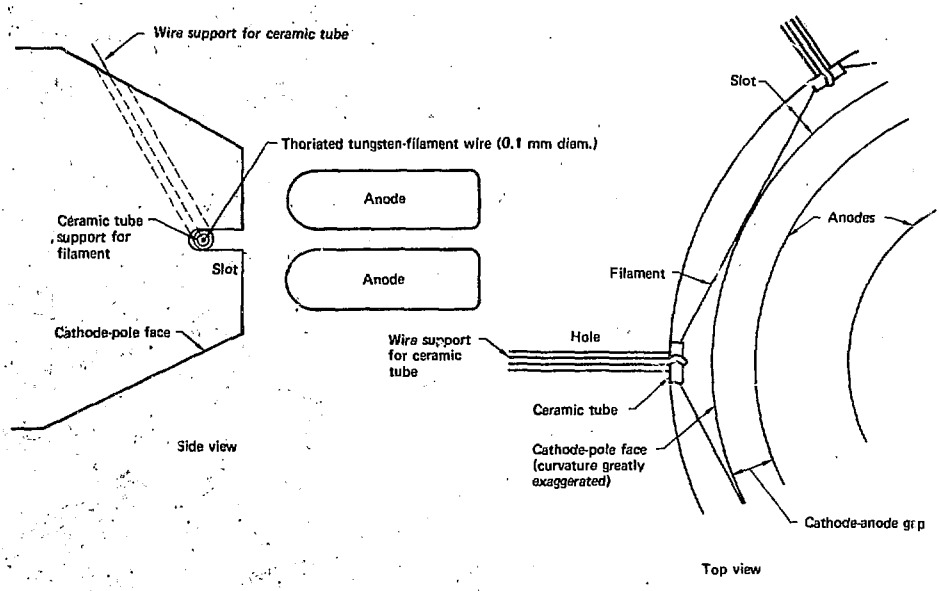

Fig. 4. Conceptual design of the electron-gun filament.

between the anodes and cathodes in this device is not expected to be a serious problem; however, holding ~300 kV in the reactor may be difficult.

Microwave heating power will be channeled in with waveguides, as illustrated in Fig. 3 [item (11)], for waves in the 10- to 20-GHz region that are resonant with the electron cyclotron frequency at the 0.36 to 0.72 T isobars. Although the wave frequency is below the central electron plasma frequency (for $n = 10^{13}$ cm^{-3}, $\omega_p/2\pi = 28$ GHz), the plasma density in the outer layers, where heating occurs, is expected to be lower, so that effective penetration can occur. If $n = 10^{13}$ cm^{-3}, $V = 1000$ cm^3, $T_e = 2$ keV, $T_i = 1$ keV, and $\tau_E = 5$ ms (a pessimistic value), then about 1 kW of heating power must be absorbed. Neutral-beam heating may prove to be one of the best heating methods. Magneto-acoustic or transit-time heating is possible, but has not been worked out.

Diagnostics

The device described in this paper is unique in that its many large access ports facilitate diagnostics. The diagnostics are listed in Table 3. Many of these techniques, although standard, have not been applied to electrostatic plugging experiments in the past because of poor access to the plasma. Diagnostics related to sheath studies, which are not standard, must be developed specially for this research.

Table 3. Diagnostics for the electrostatic plugging experiment.

Technique	Parameters
Microwave interferometer	$\int n_e dx$ diagonally through the plasma.
Thomson scattering	$n_e(x,y,z)$, $T_e(x,y,z)$.
Charge-exchange neutral-atom detector	$f(v_i)$, T_i.
Heavy ion beam probe	Potential well depth.
Spectroscopy	Impurity concentrations, T_i (impurities).
X-ray detector with variable attenuators	T_e.
Diamagnetic loops	Excluded flux, plasma pressure $n(T_e + T_i)$.
Capacitive probes	Fluctuations, diocotron oscillations, $\tilde{E}$.
Movable limiter-probe[a]	Properties of boundary plasma, thickness of boundary layer.
Currents to anodes and cathodes	Particle loss rates, total numbers of ions and electrons present.
Microwave cavity between anodes[a]	$n_e a$ (product of anode electron density and electron stream width).
CO_2 laser heterodyne system tangential to plasma boundary (with Abel inversion)[a]	$n_e(r)$ in boundary sheath.

[a]Diagnostics for sheath studies.

Alternate Geometries

The same magnetic field and plasma configuration as shown in Figs. 1 and 3 can be produced with different coil configurations; this is another advantage gained by the use of iron. Figure 5 shows one configuration in which all four coils [item (7)] have the same diameter.

Since the plasma loss rate is directly proportional to the plasma surface area, the product $n\tau$ can be increased by increasing the volume-to-area ratio. This ratio is increased by increasing the number of poles until about 10 poles, after which it levels off. The volume-to-surface ratio is about two times greater for a hexapole than for the corresponding quadrupole and about three times greater for an octapole (Fig. 6). Figure 7 shows a hexapole configuration produced by four identical coils plus two larger coils.

Conclusions

The experimental device described here should reach a regime in parameter space that is beyond other existing or planned experiments of this type. Two novel features of the new device are (1) iron is used to increase the magnetic field to 1.6 T at the anodes and to allow room for diagnostics, and (2) a toroidal

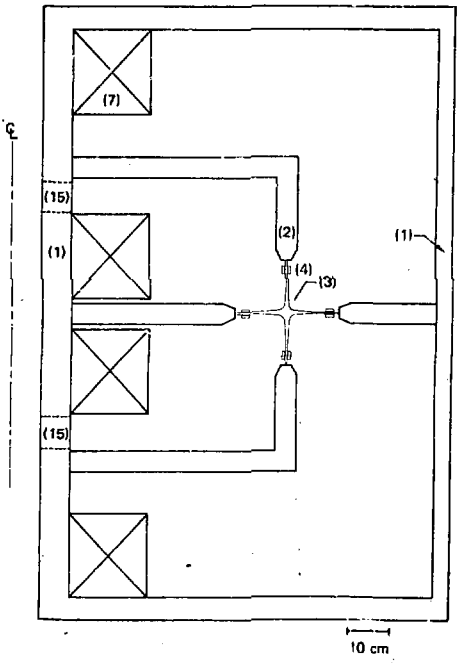

Fig. 5. Toroidal quadrupole device made with four identical coils and using iron to shape and concentrate the field. The labels are identified in the Fig. 3 caption.

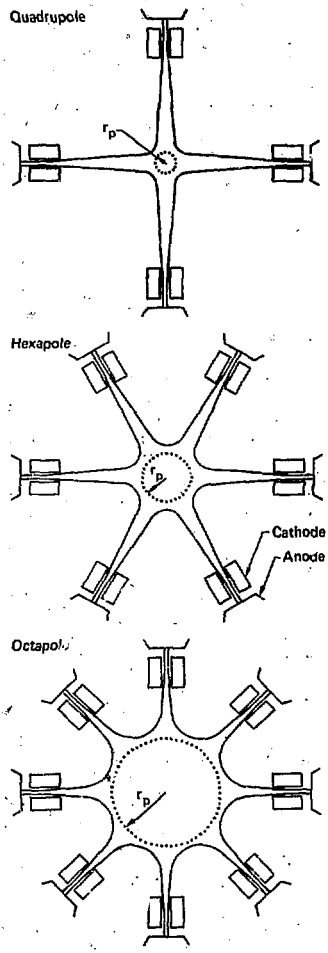

Fig. 6. The plasma volume increases as the number of poles increases; the surface area also increases, but more slowly than the volume (r_p = plasma minor radius).

rather than axial geometry is used, with the result that point cusps are eliminated and only line cusps remain. The result of (1) is that n_e will probably increase (with B^2) to 10^{13} cm^{-3}. The result of (2) is that τ_E, the energy confinement time, will probably increase to ~10 ms.

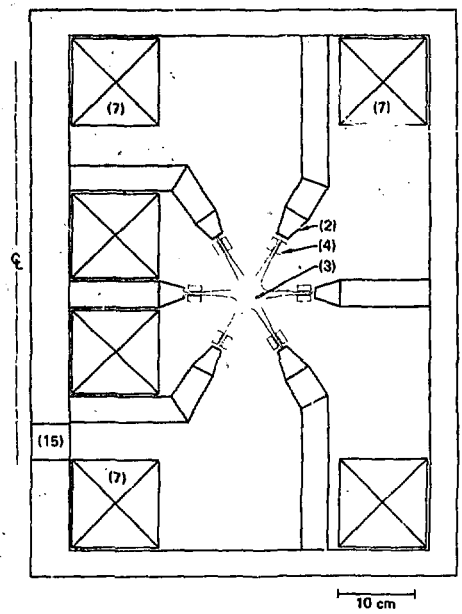

Fig. 7. Toroidal hexapole device using iron to shape and concentrate the field. The labels are identified in the Fig. 3 caption.

If scaling laws based on present experiments continue to hold as the field strength and confinement times are increased, a reactor based on this concept would look very attractive.

References

1. O. A. Lavrent'ev, "Investigation of Plasma Containment By a Magnetic Field Layer," Ukr. Fiz. Zh. 8, 446 (1963).
2. T. J. Dolan, Review of Electrostatic Plugging, Lawrence Livermore Laboratory, Rept. UCID-17576 (1977).
3. R. W. Moir, A New Magnetic Well Configuration, Importance of the Mirror Ratio, and Electrostatic Containment of Warm Plasma, EURATOM Rept. EUR-CEA-FC-496, Fontenay-Aux-Roses, France (1968).
4. T. J. Dolan, Design Study of Electrostatically Plugged Cusp Fusion Reactor, Lawrence Livermore Laboratory, Rept. UCRL-52142 (1976).

NOTICE

"This report was prepared as an account of work sponsored by the United States Government. Neither the United States nor the United States Energy Research & Development Administration, nor any of their employees, nor any of their contractors, subcontractors, or their employees, makes any warranty, express or implied, or assumes any legal liability or responsibility for the accuracy, completeness or usefulness of any information, apparatus, product or process disclosed, or represents that its use would not infringe privately-owned rights."

CKM/jcn/jy/mla